Title: **Involvement of vesicular trafficking system in membrane targeting of the progeny influenza virus genome**

Authors: Shuichi Jo[a, 1], Atsushi Kawaguchi[a, b, 1], Naoki Takizawa[c], Yuko Morikawa[b], Fumitaka Momose[b, *], Kyosuke Nagata[a, *]

Affiliations: [a]Department of Infection Biology, Graduate School of Comprehensive Human Sciences, University of Tsukuba, 1-1-1 Tennodai, Tsukuba 305-8575, Japan

[b]Kitasato Institute for Life Sciences, Kitasato University, 5-9-1 Shirokane, Minato-ku, Tokyo 108-8641, Japan

[c]Graduate School of Biomedical Sciences, University of Nagasaki, 1-14 Bunkyo, Nagasaki 852-8521, Japan

[1]These authors contributed equally to this article.

* Corresponding authors:

Mailing address: Kyosuke Nagata, Department of Infection Biology, Graduate School of Comprehensive Human Sciences, University of Tsukuba, 1-1-1 Tennodai, Tsukuba 305-8575, Japan. Phone: +81 (298) 53-3233. Fax: +81 (298) 53-3233. E-mail: knagata@md.tsukuba.ac.jp.

Mailing address: Fumitaka Momose, Kitasato Institute for Life Sciences, Kitasato University, 5-9-1 Shirokane, Minato-ku, Tokyo 108-8641, Japan. Phone: +81 (3) 5791-6268. Fax: +81 (3) 5791-6268. E-mail: fmomose@lisci.kitasato-u.ac.jp.

**Abstract**

**The genome of influenza type A virus consists of single-stranded RNAs of negative polarity. Progeny viral RNA (vRNA) replicated in the nucleus is nuclear-exported, and finally transported to the budding site beneath the plasma membrane. However, the precise process of the membrane targeting of vRNA is unclear, although viral proteins and cytoskeleton are thought to play roles. Here, we have visualized the translocation process of progeny vRNA using fluorescence in situ hybridization method. Our results provide an evidence of the involvement of vesicular trafficking in membrane targeting of progeny vRNA independent of that of viral membrane proteins.**

Keywords: influenza virus; vesicular trafficking; ribonucleoprotein; fluorescence in situ hybridization

## 1. Introduction

Influenza type A virus possesses eight-segmented and single-stranded RNAs of negative polarity (vRNA) as its genome. Progeny vRNA is replicated through complementary RNA (cRNA) in the nucleus [1]. The replicated vRNA forms ribonucleoprotein complexes (designated vRNP) with viral RNA polymerase proteins (PB1, PB2, and PA) and NP [2]. Progeny vRNP is exported from the nucleus through the CRM1-dependent pathway by the interaction with M1 and NS2 [3-6]. After the nuclear export, the progeny vRNP reaches the budding site beneath the cell surface, and finally a set of eight segments of vRNA is incorporated into a progeny virion with other viral structural proteins, HA, NA, and M2 on the apical plasma membrane [7-9]. The distribution of viral transmembrane proteins on the apical plasma membrane is believed to determine the budding site of progeny virion [8, 9]. These viral membrane-associating proteins are targeted to plasma membrane domains by an exocytic pathway through the *trans*-Golgi network (TGN). Although the apical sorting signal of M2 is yet to be defined, HA, NA, and M2 possess the determinants for sorting and targeting to the apical plasma membrane [9]. Previously, it is suggested that either viral factors, HA, NA, and M1, or cytoskeleton elements are involved in the transport of vRNP to the cell surface [9]. Since M1, is a major viral membrane-associated protein, interacts with vRNP and the cytoplasmic domain of HA [10-12], it is speculated that vRNP might be tethered to the lipid vesicles associated with HA and/or NA during the exocytic event via their interaction with M1 [10-12]. However, a genetically engineered virus encoding HA lacking its cytoplasmic tail, which is a putative M1-interacting domain, hardly reduced the efficiency of virus production [13]. It is reported that influenza viruses carrying a mutant HA with a basolateral sorting signal are assembled at apical plasma membrane [14, 15]. Similarly, NA is also shown not to be required for virus assembly and budding [16]. Furthermore, it is proposed that vRNP is transported to apical plasma membrane by itself since NP has intrinsic apical targeting activity [17]. Therefore, the transport mechanism of progeny vRNP to apical membrane, including the responsible cellular compartment(s), is still not conclusive.

Here, we visualized the intracellular localization of vRNA in infected cells, in order to clarify the mechanism of its cytoplasmic localization and membrane targeting. We found that the newly synthesized vRNA is localized in a juxta-nuclear region of the cytoplasm of infected cells. The cytoplasmic vRNA showed similar staining pattern with organelles responsible for the vesicular trafficking and appeared to be re-distributed in the presence of potent inhibitors of the vesicular trafficking. However, the intracellular localization of HA and M1 hardly merged with that of progeny vRNA in the absence or presence of inhibitors of the vesicular trafficking. Our results provide an evidence of the involvement of vesicular trafficking tethered onto the cytoskeleton in localization and membrane targeting of vRNA, which is independent of the transport pathway of HA and M1.

## 2. Materials and methods

### *2.1. Indirect immunofluorescence assay*

MDCK cells grown on coverslips were rinsed shortly by 4% paraformaldehyde (PFA) in PBS, and then pre-permeablized with cold-0.25% Triton X-100 in CSK buffer (200 mM pipes [pH 6.8], 0.25% [v/v] Triton X-100, 100 mM NaCl, 300 mM Sucrose, 3 mM $MgCl_2$, 1 mM EGTA) for 3 min on ice. After being rinsed with CSK buffer, cells were fixed by 4% PFA in PBS for 10 min at room temperature, and then permeabilized with 0.5% Triton X-100 in PBS for 5 min on ice. Coverslips were soaked in 1% nonfat dry milk in PBS for 1 h, and then incubated for 1 h with antibodies where indicated. After wash with 0.1% (v/v) Tween-20 in PBS, coverslips were incubated with Alexa Flour 568-conjugated anti-mouse or -rabbit IgG (Invitrogen) for 1 h. Images were acquired by confocal laser-scanning microscope (Zeiss).

### *2.2. FISH assay*

After the indirect immunofluorescence assays, cells were fixed in 4% PFA for 10 min, and permeabilized on ice with 0.5% Triton X-100 in PBS for 5 min. After deproteinization by incubating at room temperature with 0.2 μg/ml of Proteinase K (ProK) in PBS containing 0.1% Tween-20 for 5 min, cells were re-fixed in 4% PFA for 10 min, and then subjected to stepwise dehydration in ice-cold 70, 90, and 99.5% ethanol. The dried coverslips were incubated with a biotin-labeled RNA probe, which was denatured in a buffer containing 20 mM $NaHCO_3$ and 30 mM $Na_2CO_3$ at 60˚C for 40 min and neutralized by adding equal volume of 3 M sodium acetate containing 1% acetic acid, for 12 h at 37˚C. After hybridization, cells were washed with 2x SSC containing 50% formamide and subsequently with 2x SSC at 42˚C. The coverslips were soaked in 5% BSA in 4x SSC containing 0.1% Tween-20 for 30 min at 37˚C, and further incubated with 10 μg/ml of avidin-FITC (invitrogen) in 4x SSC containing 0.1% Tween-20 for 30 min at 37˚C. After being washed with 4x SSC containing 0.1% Tween-20 at 42˚C, cells were examined by confocal laser-scanning microscope (Zeiss).

## 3. Results and discussion

### *3.1. Visualization of the influenza virus genome by FISH method*

We examined the localization of vRNA with progression of infection by FISH assays. FISH assays were carried out essentially as previously reported [18] except for deproteinization with 0.2 μg/ml of Proteinase K. The signals of vRNA appeared from 4 hours post infection (hpi) in the nucleus, where the genome replication takes place (Fig. 1). Since no signal was found until 2 hpi, the signals detected by the FISH method are not due to the incoming vRNA. The strong granular signals were localized around the nucleus at 6 hpi, whereas these granules were expanded in the entire cytoplasm with a unique organelle-like distribution pattern after 8 hpi (Fig. 1). We also found that the cytoplasmic granules are not formed even at 12 hpi in the presence of leptomycin B, a potent inhibitor of CRM1 (data not shown). These indicate that the FISH signals represent the intracellular localization of newly synthesized vRNA exported from nucleus. The same results were obtained for other segments (data not shown).

Further to confirm whether these vRNAs in granules form vRNP complexes, we counterstained NP. In order to detect NP bound to vRNA, we performed the indirect immunofluorescence assay using a monoclonal anti-NP antibody, mAb61A5, which preferentially recognizes NP on vRNP complexes [19]. Figure 1 indicates that most of FISH signals as cytoplasmic granules are co-localized with NP bound to vRNA. Therefore, we conclude that the vRNA in cytoplasmic granules form vRNP complexes. The vRNP visualized here could be destined to be packaged into new virus particles since we also observed the vRNP beneath the apical plasma membrane with HA in cells fixed with 4% PFA at 6 hpi but not 4 hpi (Supplementary fig. 1).

*3.2. The localizatioin of vRNP at cellular organelles involved in vesicular trafficking*

To reveal a cellular compartment(s), in which newly synthesized vRNA accumulates, we observed the localization of cellular organelle by immunostaining using antibodies against marker proteins: Calnexin is a marker protein for endoplasmic reticulum; Furin for TGN; EEA1 for early endosome; and M6PR for late endosome (Fig. 2). The distribution pattern of vRNA was found similar to that of these organelles. However, the majority of the vRNA was not co-localized with ER, early endosome, and late endosome, although a part of vRNA was merged with these organelles. In contrast, a distinct portion of vRNA was co-localized with the TGN. Exactly the same results were observed by using anti-NP antibody, mAb61A5 (data not shown). In addition, we also found that vRNP is partially localized with microtubules including the microtubule organizing center (data not shown). These results strongly suggest the involvement of the vesicular trafficking system in the membrane targeting of vRNP along cytoskeleton.

*3.3. Intracellular localization of HA and M1 with vRNP*

Previously, it is speculated that M1, a major viral membrane-associated matrix protein, tethers vRNP to the exocytic membrane associated with HA and/or NA [10-12]. To address this, the localization of HA and M1 was compared with that of newly synthesized vRNA (Fig. 3A and 3B). Along with the progression of infection, HA and M1 became present as cytoplasmic granules from 6 hpi as did newly synthesized vRNA (Fig. 3A and 3B). However, only a small fraction of HA or M1 was co-localized with vRNA. This suggests that only a small fraction of vRNP interacts with exocytic vesicles associated with HA and/or M1 and progeny vRNP is transported to the plasma membrane through a trafficking pathway independent of that for HA and M1.

*3.4. The effect of Golgi-disturbing agents on the localization of vRNA and viral proteins*

The TGN is responsible for the transport of membrane proteins and lipid from ER to more distal compartments. The delivery of transport vesicles from TGN to plasma membrane undergoes with a high fidelity, which could be guaranteed by vesicles targeting along cytoskeleton. Previous studies showed the interaction of NP and M1 with cytoskeletal components [20, 21] and the co-localization of NP with microtubule [19]. To reveal the relationship between vesicular trafficking and membrane targeting of progeny vRNP, the localization of vRNA was examined upon the treatment with either nocodazole or brefeldin A. Nocodazole disrupts polymerization of microtubule and causes fragmentation of TGN, while brefeldin A, a potent inhibitor of the vesicle formation, causes formation of an extensive TGN tubular network [22]. Therefore, if vRNA is associated with the vesicular trafficking system, the localization of vRNA might be re-located by the addition of nocodazole and brefeldin A. FISH assays were applied to infected cells treated with nocodazole or brefelidin A. Fragmented foci and tubular localization of vRNA were found in the cytoplasm in the presence of nocodazole and brefeldin A, respectively (Fig. 3C). High resolution images were provided in Supplementary fig. 2. The patterns of tubular vRNP structures found upon BFA treatment were reminiscent of microtubule staining. However, vRNP was co-localized partially with microtubule in the absence or presence of BFA (Supplementary fig. 3). These results suggest the possible correlation between the vesicular trafficking system and membrane transport of newly synthesized vRNP. After the treatment with nocodazole or brefeldin A, newly synthesized vRNA was hardly found to be co-localized with HA or M1 (Fig. 3C). These results strongly suggest that the transport pathway of progeny vRNP in the cytoplasm could be different from that of HA or M1, both of which are thought to be membrane-targeted through the vesicular trafficking system [9, 12]. It is quite likely that the major portion of vRNP is targeted to the plasma membrane using an exocytic pathway independent of HA and M1, although we cannot completely exclude the possibility of the involvement of HA and M1 in vRNP transport. Further to clarify the mechanism of vRNP transport to the apical membrane, identification of a cellular factor(s) involved in the vRNP transport is critical.

**Acknowledgements**

This work was supported in part by a grant-in-aid from the Ministry of Education, Culture, Sports, Science, and Technology of Japan (to K.N., F.M., and Y.M.), Research Fellowship of the Japanese Society for the Promotion of Science (JSPS) (to A.K.), and Kitasato University Research Grant for Young Researchers (to F.M.)

**References**

[1] K. Nagata, A. Kawaguchi, T. Naito, Host factors for replication and transcription of the influenza virus genome, Rev Med Virol 18 (2008) 247-260.

[2] A. Portela, P. Digard, The influenza virus nucleoprotein: a multifunctional RNA-binding protein pivotal to virus replication, J Gen Virol 83 (2002) 723-734.

[3] D. Elton, M. Simpson-Holley, K. Archer, L. Medcalf, R. Hallam, J. McCauley, P. Digard, Interaction of the influenza virus nucleoprotein with the cellular CRM1-mediated nuclear export pathway, J Virol 75 (2001) 408-419.

[4] G. Neumann, M.T. Hughes, Y. Kawaoka, Influenza A virus NS2 protein mediates vRNP nuclear export through NES-independent interaction with hCRM1, Embo J 19 (2000) 6751-6758.

[5] R.E. O'Neill, J. Talon, P. Palese, The influenza virus NEP (NS2 protein) mediates the nuclear export of viral ribonucleoproteins, Embo J 17 (1998) 288-296.

[6] K. Watanabe, N. Takizawa, M. Katoh, K. Hoshida, N. Kobayashi, K. Nagata, Inhibition of nuclear export of ribonucleoprotein complexes of influenza virus by leptomycin B, Virus Res 77 (2001) 31-42.

[7] T. Noda, H. Sagara, A. Yen, A. Takada, H. Kida, R.H. Cheng, Y. Kawaoka, Architecture of ribonucleoprotein complexes in influenza A virus particles, Nature 439 (2006) 490-492.

[8] J. Zhang, A. Pekosz, R.A. Lamb, Influenza virus assembly and lipid raft microdomains: a role for the cytoplasmic tails of the spike glycoproteins, J Virol 74 (2000) 4634-4644.

[9] D.P. Nayak, E.K. Hui, S. Barman, Assembly and budding of influenza virus, Virus Res 106 (2004) 147-165.

[10] X. Huang, T. Liu, J. Muller, R.A. Levandowski, Z. Ye, Effect of influenza virus matrix protein and viral RNA on ribonucleoprotein formation and nuclear export, Virology 287 (2001) 405-416.

[11] H. Zhao, M. Ekstrom, H. Garoff, The M1 and NP proteins of influenza A virus form homo- but not heterooligomeric complexes when coexpressed in BHK-21 cells, J Gen Virol 79 ( Pt 10) (1998) 2435-2446.

[12] A. Ali, R.T. Avalos, E. Ponimaskin, D.P. Nayak, Influenza virus assembly: effect of influenza virus glycoproteins on the membrane association of M1 protein, J Virol 74 (2000) 8709-8719.

[13] H. Jin, G.P. Leser, R.A. Lamb, The influenza virus hemagglutinin cytoplasmic tail is not essential for virus assembly or infectivity, Embo J 13 (1994) 5504-5515.

[14] R. Mora, E. Rodriguez-Boulan, P. Palese, A. Garcia-Sastre, Apical budding of a recombinant influenza A virus expressing a hemagglutinin protein with a basolateral localization signal, J Virol 76 (2002) 3544-3553.

[15] S. Barman, L. Adhikary, Y. Kawaoka, D.P. Nayak, Influenza A virus hemagglutinin containing basolateral localization signal does not alter the apical budding of a recombinant influenza A virus in

polarized MDCK cells, Virology 305 (2003) 138-152.

[16] C. Liu, M.C. Eichelberger, R.W. Compans, G.M. Air, Influenza type A virus neuraminidase does not play a role in viral entry, replication, assembly, or budding, J Virol 69 (1995) 1099-1106.

[17] M. Carrasco, M.J. Amorim, P. Digard, Lipid raft-dependent targeting of the influenza A virus nucleoprotein to the apical plasma membrane, Traffic 5 (2004) 979-992.

[18] R. Singer, Subcellular localization of genes and their products, in: G.R. Spector DL., Leinwand LA. (Ed.), Cells: a laboratory manual, Cold spring harbor laboratory press, 1998, pp. 116.111-116.116.

[19] F. Momose, Y. Kikuchi, K. Komase, Y. Morikawa, Visualization of microtubule-mediated transport of influenza viral progeny ribonucleoprotein, Microbes Infect 9 (2007) 1422-1433.

[20] P. Digard, D. Elton, K. Bishop, E. Medcalf, A. Weeds, B. Pope, Modulation of nuclear localization of the influenza virus nucleoprotein through interaction with actin filaments, J Virol 73 (1999) 2222-2231.

[21] R.T. Avalos, Z. Yu, D.P. Nayak, Association of influenza virus NP and M1 proteins with cellular cytoskeletal elements in influenza virus-infected cells, J Virol 71 (1997) 2947-2958.

[22] A. Dinter, E.G. Berger, Golgi-disturbing agents, Histochem Cell Biol 109 (1998) 571-590.

**Legends of figures**

Fig. 1. The intracellular localization of vRNP. MDCK cells were mock-infected or infected with influenza virus PR/8/34 strain at moi of 10. At 2, 4, 6, 8, and 12 hpi, infected MDCK cells were subjected to indirect immunofluorescence assays using anti-NP antibody (mAb61A5, red). vRNA was also detected by the FISH method using an RNA probe complementary to the segment 1 vRNA (green). Magnified image was shown in the window at 6 hpi. All images were captured at the equal laser intensity and under the same exposure time by confocal laser-scanning microscope.

Fig. 2. The distribution of cellular organelle marker proteins and vRNP. At 8 hpi, infected cells were subjected to indirect immunofluorescence assays using anti-Calnexin (ER, red), anti-Furin (TGN, red), anti-EEA1 (early endosome, red), and anti-M6PR (late endosome, red) antibodies, respectively, and then vRNA was visualized by the FISH method (green). Magnified images were shown in the windows.

Fig. 3. The localization of vRNA and viral proteins. (A and B) Intracellular localization of HA and M1 with vRNP. Infected cells were subjected to indirect immunofluorescence assays with either anti-HA (panel A, red) or anti-M1 (panel B, red) antibodies, and then FISH assays to visualize vRNA (green). Magnified images were also shown in the windows at 6 hpi for HA, and at 8 hpi for M1. All images were captured at the equal laser intensity and under the same exposure time by confocal laser-scanning microscope. (C) The effect of Golgi-disturbing agents on the localization of vRNA and viral proteins. At 7 hpi, infected cells were incubated for 1 h in the presence of either DMSO, 1 μg/ml Nocodazole (Noc), or 28 μg/ml brefeldin A (BFA). HA (left panel, red) and M1 (right panel, red) were detected using either anti-HA and anti-M1 antibodies,

respectively, and then vRNA was visualized by the FISH method (green).

Figure 1 Jo S. et al

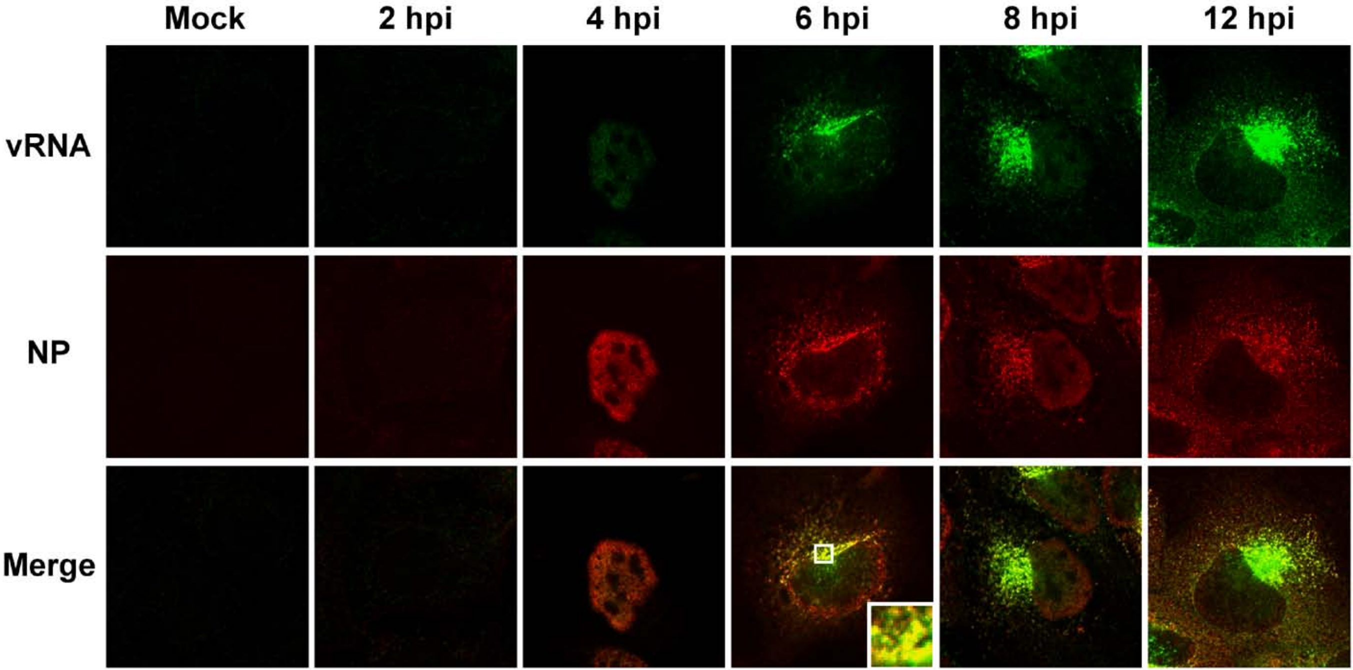

Figure 2 Jo S. et al

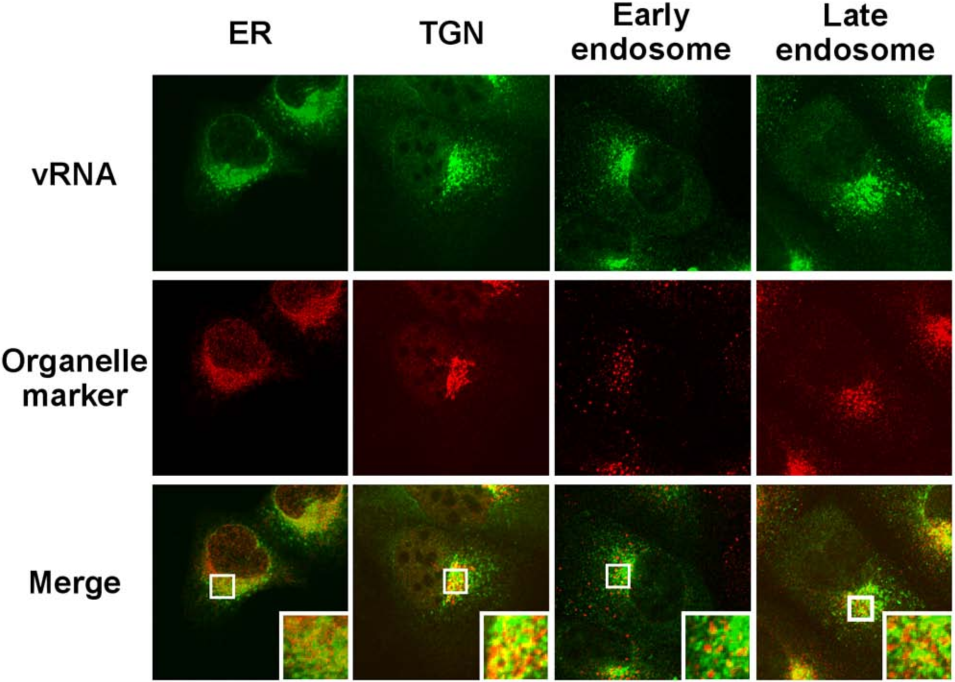

Figure 3A and 3B Jo S. et al

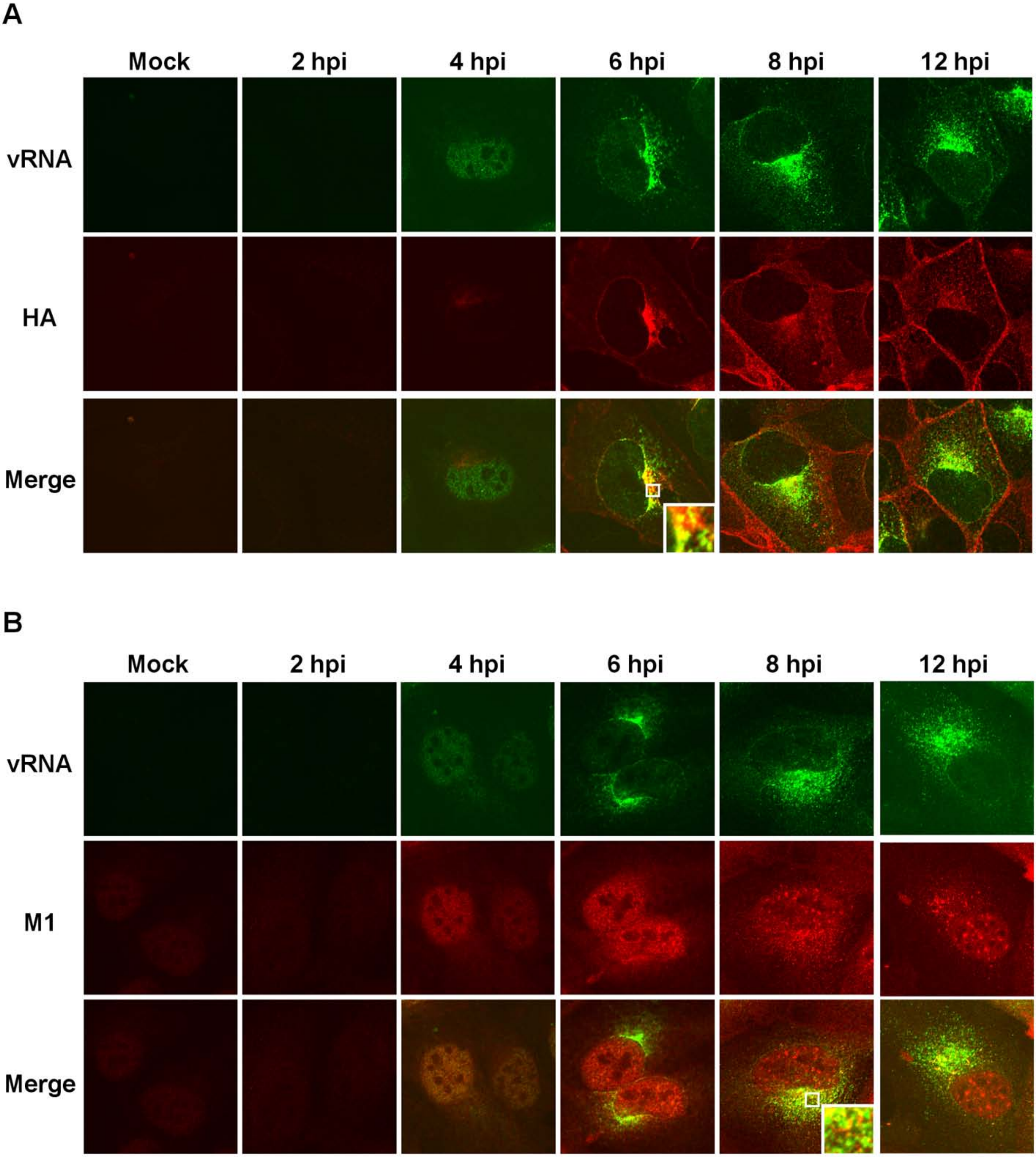

Figure 3C Jo S. et al

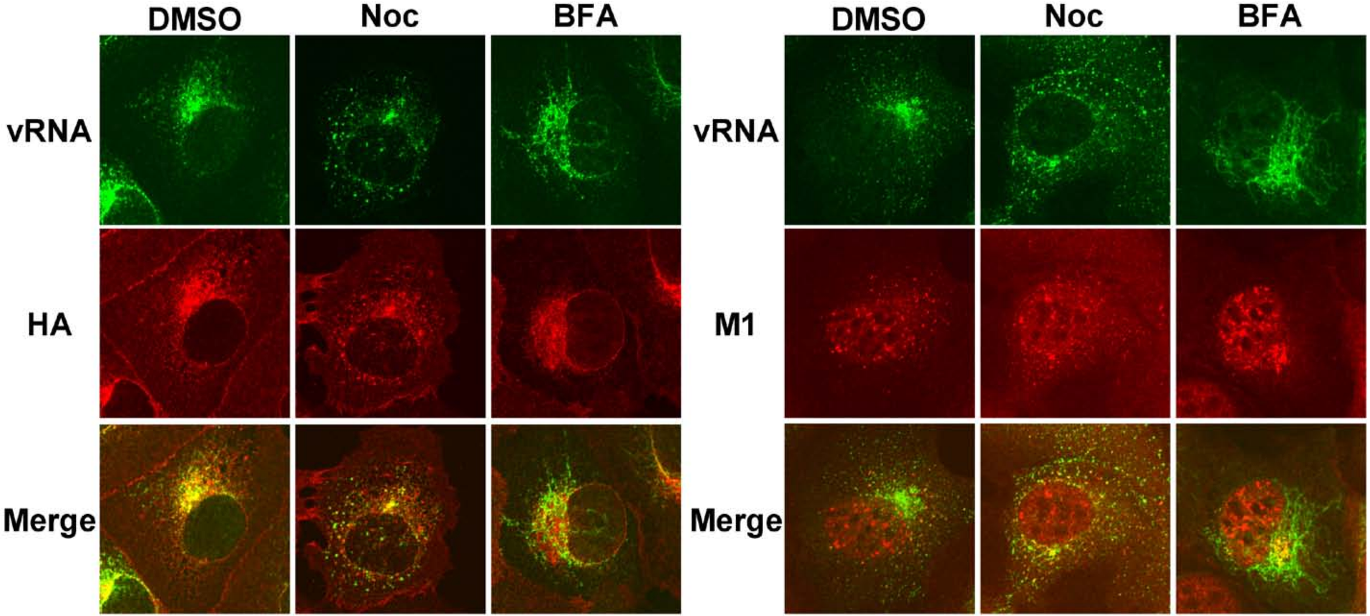

## Supplementary text

## Materials and Methods

*Biological materials*

Madin-Darby canine kidney (MDCK) cells were grown in minimum essential medium (MEM) (Nissui) containing 10% of fetal bovine serum. MDCK cells were infected with influenza virus (A/Puerto Rico/8/34) at multiplicity of infection (moi) of 10 PFU/cell. After incubation for 1 h, cells were washed and maintained in serum-free MEM.

Anti-NP (mAb61A5) [1], anti-HA (C-179, TAKARA), anti-M1 [2, 3], anti-Calnexin (Stressgen), anti-Furin (Affinitiy Bio Reagents), anti-Early endosome antigen 1 (EEA1, Becton Dickinson), and anti-Mannose 6 phosphate receptor (M6PR, Abcam) antibodies were used in immunofluorescence assays.

*Preparation of fluorescence in situ hybridization (FISH) probe*

A single-stranded RNA, which is complementary to the segment 1 vRNA between nucleotide sequence positions 1268 and 2341, was synthesized using RiboMAX$^{TM}$ Large Scale RNA Production System (Promega) for a probe of FISH assay. Briefly, PCR product, which was amplified from cDNA of segment 1 with specific primers 5’-TAATACGACTCACTATAGGGAGCAAAAGCAGG-3’ and 5’-AAGATTGCCCGTAAGCACCTCTT-3’, was transcribed by T7 RNA polymerase in the presence of 0.35 mM Biotin-16-UTP (Roche) for 12 h at 37˚C. The RNA product was digested by DNase I (Promega) at 37˚C for 30 min, then purified by RNeasy Mini Kit (QIAGEN) according to the manufacture’s procedure. Purified RNA was partially hydrolyzed in a buffer containing 20 mM $NaHCO_3$ and 30 mM $Na_2CO_3$ at 60˚C for 40 min, and then neutralized by adding equal volume of 3 M sodium acetate containing 1% acetic acid. Further, the digested RNA probe was precipitated with ethanol in the presence of salmon sperm DNA and yeast tRNA, and then resolved in a solution containing 2x SSC, 50% formamide, and 10% dextran sulfate.

## References

[1] F. Momose, Y. Kikuchi, K. Komase, Y. Morikawa, Visualization of microtubule-mediated transport of influenza viral progeny ribonucleoprotein, Microbes Infect 9 (2007) 1422-1433.

[2] K. Watanabe, H. Handa, K. Mizumoto, K. Nagata, Mechanism for inhibition of influenza virus RNA polymerase activity by matrix protein, J Virol 70 (1996) 241-247.

[3] K. Watanabe, N. Takizawa, M. Katoh, K. Hoshida, N. Kobayashi, K. Nagata, Inhibition of nuclear export of ribonucleoprotein complexes of influenza virus by leptomycin B, Virus Res 77 (2001) 31-42.

Supplementary fig. 1. Visualization of vRNP and HA beneath apical plasma membrane using Z-axis reconstitution. Infected MDCK cells were fixed in 4% PFA at 4 (upper panels) or 6 hpi (lower panels). Immunofluorescence staining was carried out with anti-HA (red), anti-ZO-3 as a tight junction marker (blue; Invitrogen), and Alexa Fluor 488-conjugated anti-NP (green; mAb61A5) antibodies, and then cells were examined using confocal laser-scanning microscopy. Images were obtained either as xy plane (upper panel) or xz plane sections along the indicated dotted line in xy-plane images (lower panel) in each time point post infection. The vRNP were found beneath apical plasma membrane with HA at 6 hpi but not at 4 hpi.

Supplementary fig. 2. High resolution images for the localization of vRNP in the presence of Golgi-disturbing agents. At 7 hpi, infected cells were incubated for 1 h in the presence of DMSO, 1 μg/ml Nocodazole, or 28 μg/ml brefeldin A (BFA) and then subjected to FISH assays. DNA was counterstained with TO-PRO-3 (blue).

Supplementary fig. 3. The intracellular localization of vRNP and microtubule in the presence of BFA. At 7 hpi, infected cells were incubated for 1 h in the presence of 28 μg/ml BFA and then subjected to indirect immunofluorescence assays with anti-NP (green; mAb61A5) and anti-α-tubulin (red; Sigma Aldrich) antibodies. Enlarged images of the indicated area (white box) are also shown. The tubular structures of vRNP partially co-localized with microtubule in the presence of BFA.

Supplementary figure 1  Jo S. et al

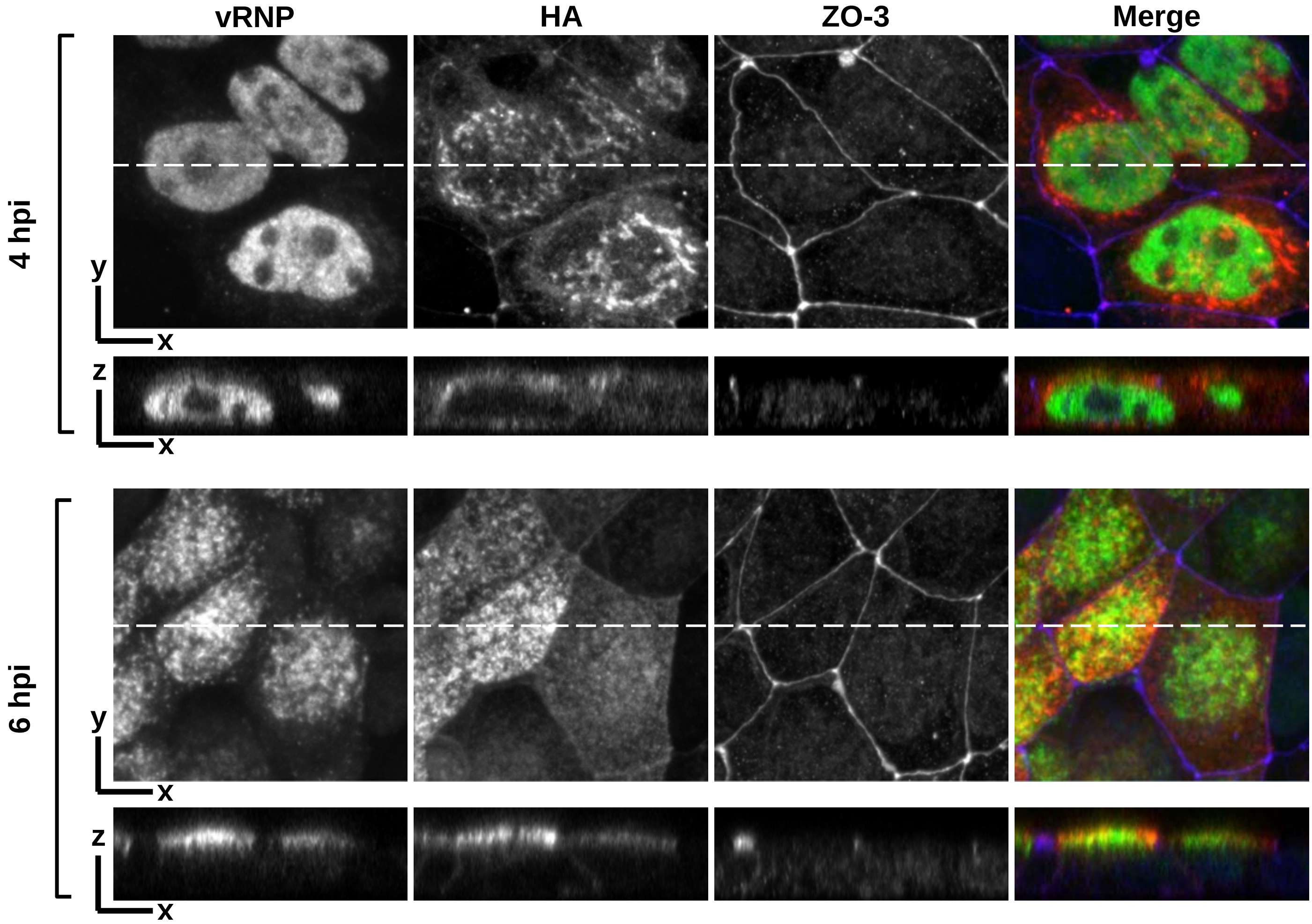

**Supplementary figure 2  Jo S. et al**

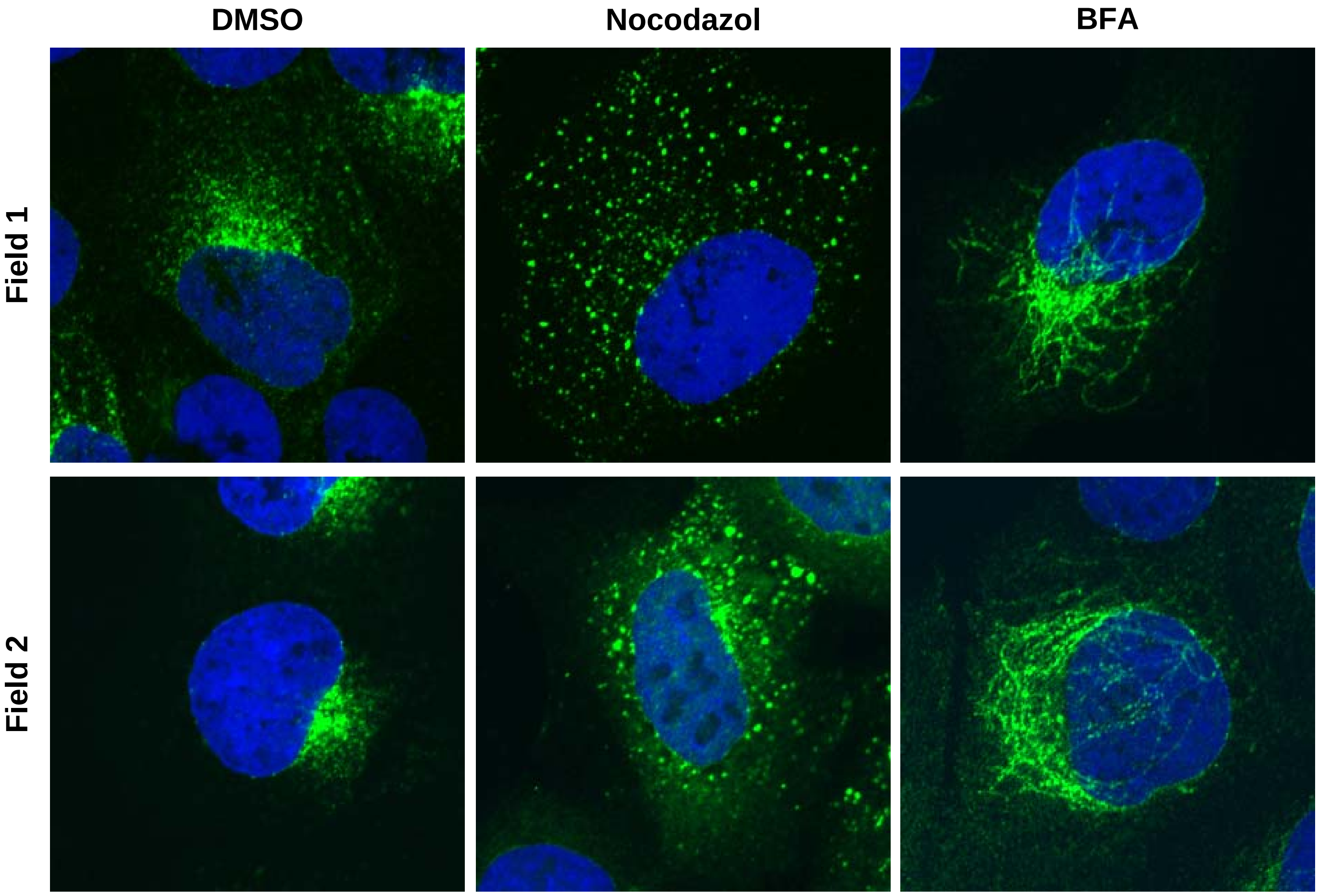

**Supplementary figure 3  Jo S. et al**